© 2019. Published by The Company of Biologists Ltd | Journal of Experimental Biology (2019) 222, jeb198291. doi:10.1242/jeb.198291

RESEARCH ARTICLE

Cranial kinesis in the miniaturised lizard *Ablepharus kitaibelii* (Squamata: Scincidae)

Stephan Handschuh[1,*], Nikolay Natchev[2], Stefan Kummer[1], Christian J. Beisser[3], Patrick Lemell[3], Anthony Herrel[4] and Vladislav Vergilov[5]

ABSTRACT

Cranial kinesis refers to intracranial movements in the vertebrate skull that do not concern the jaw joint, the middle ear or the hypobranchial skeleton. Different kinds of cranial kinesis have been reported for lizards, including mesokinesis, metakinesis, amphikinesis (simultaneous mesokinesis and metakinesis) and streptostyly. Streptostyly is considered relatively widespread within lizards, whereas mesokinesis has been documented only for geckos, varanids and anguids. The present study investigated cranial kinesis in the miniaturised scincid *Ablepharus kitaibelii* by integrating morphological and experimental data. Based on micro computed tomography, we provide a description of skull osteology. Cranial joints were studied with histology, which results in the first detailed description of cranial joint histology for a member of the Scincidae. Taken together, the morphological data indicate a high potential for amphikinesis and streptostyly, which was also corroborated by skull manipulations. High-speed cinematography demonstrated that mesokinesis occurs during food uptake, processing and intraoral transport cycles. Bite force measurements showed prolonged and reasonably hard biting even at large gape angles. Based on these data, we formulate a model of the amphikinetic *A. kitaibelii* skull mechanism, which provides an extension of Frazzetta's quadric-crank model by placing a special emphasis on metakinesis. According to this model, we hypothesise that metakinetic intracranial movements may provide a means for reducing strain in jaw adductor muscles. Presented hypotheses can be addressed and tested in future studies.

KEY WORDS: Metakinesis, Mesokinesis, Amphikinesis, Streptostyly, MicroCT, Feeding, Functional morphology, Cinematography, Bite force

INTRODUCTION

Cranial kinesis – intracranial movements in the vertebrate skull that are unrelated to the jaw joint, the middle ear or the hypobranchial skeleton – is found in several groups of extant Sauropsida, including birds within the Archosauria (Bock, 1964; Zusi, 1993; Zweers, 1982), as well as ophidians (snakes) and non-ophidian squamates (lizards) within the Lepidosauria (Frazzetta, 1962, 1966; Gans, 1961; Herrel et al., 1999; Kardong, 1977; Metzger, 2002; Rieppel, 1993). Considerations on cranial kinesis in lizards go back to the works of Versluys early in the 20th century (Versluys, 1910, 1912, 1936), and since then this topic has received considerable interest. In a seminal work, Frazzetta (1962) developed the quadric-crank model for lizard cranial kinesis during mouth opening and mouth closing, functionally integrating three types of kinesis: metakinesis, which is movement between the braincase and dermal bones of the skull roof; mesokinesis, which is dorsal extension and ventral flexion of the snout around a transverse axis behind the eye; and streptostyly, which is the pendulum-like rotation of the quadrate bones allowing the position of the jaw joint to move forward and backward (for a review, see Metzger, 2002). Simultaneous metakinesis and mesokinesis is termed amphikinesis (Frazzetta, 1962; Versluys, 1912).

Since the introduction of Frazzetta's model, research on lizard cranial kinesis has focused on two main questions. (1) What kind of kinesis occurs in different squamate taxa? More specifically, does the quadric-crank model apply to a large number or even the majority of lizards? (2) What functional implications and possible adaptive value does a specific kinetic mechanism have? Concerning the documentation of presence/absence, type and magnitude of cranial kinesis, researchers have used two different approaches. On the one hand, they searched for morphological correlates of cranial kinesis in skull bones and cranial joints and investigated the mobility of skull joints based on skull manipulations on ligamentous specimens (Frazzetta, 1962; Iordansky, 1996). On the other hand, experimental approaches were utilized to investigate the presence of cranial kinesis in living animals, including conventional and high-speed cinematography (Frazzetta, 1962, 1983; Iordansky, 1966), cineradiography (Herrel et al., 1998, 1999; Herrel and De Vree, 1999; Rieppel, 1978b; Smith, 1980, 1982; Throckmorton, 1976), X-ray reconstruction of moving morphology (Montuelle and Williams, 2015), analysis of muscle activity patterns by electromyography (De Vree and Gans, 1987; Herrel et al., 1999; McBrayer and White, 2002; Smith, 1982), and studies of tensile and compressive forces in skull joints (Smith and Hylander, 1985). The sum of these approaches produced a bulk of knowledge, suggesting that streptostyly is relatively widespread among lizards and mesokinesis occurs at least in some geckos, varanids and anguids. Considerable variation in the patterns of cranial kinesis exists, however, including streptostyly without any other type of kinesis, coupled streptostyly–mesokinesis, and concurrent streptostyly–mesokinesis without functional coupling (for a review, see Metzger, 2002). Furthermore, within most species, young animals are more kinetic than older animals (Starck, 1979, A.H. personal observation). Concerning the functional implications and adaptive advantages of cranial kinesis, data indicate that large differences exist between squamate taxa. A number of hypotheses for the functional significance of mesokinesis (Condon, 1987; De Vree and Gans, 1994; Frazzetta, 1962; Herrel et al., 2000; Montuelle and Williams, 2015; Rieppel, 1979; Schwenk, 2000) and

[1]VetCore Facility for Research/Imaging Unit, University of Veterinary Medicine Vienna, Veterinaerplatz 1, Vienna 1210, Austria. [2]Department Biology, Faculty of Natural Sciences, Shumen University, Universitetska 115, 9700 Shumen, Bulgaria. [3]Department for Integrative Zoology, University of Vienna, Althanstrasse 14, Vienna 1090, Austria. [4]UMR 7179 C.N.R.S/M.N.H.N., Département Adaptations du Vivant, Bâtiment d'Anatomie Comparée, 55 rue Buffon, Paris 75005, France. [5]National Museum of Natural History, Bulgarian Academy of Sciences, 1 Tsar Osvoboditel Blvd, Sofia 1000, Bulgaria.

*Author for correspondence (stephan.handschuh@vetmeduni.ac.at)

S.H., 0000-0002-2140-7892; A.H., 0000-0003-0991-4434

Received 21 December 2018; Accepted 2 April 2019

streptostyly (Gingerich, 1971; Herrel and De Vree, 1999; MacLean, 1974; Rieppel, 1978b; Smith, 1980; Throckmorton, 1976) have been presented, and some of them were corroborated by experimental data (Metzger, 2002). Yet, no all-encompassing general hypothesis has been accepted for the functional advantage of either mesokinesis or streptostyly (Metzger, 2002).

Thus far, metakinesis has received much less attention compared with mesokinesis and streptostyly. Versluys (1910, 1912, 1936) coined the term metakinesis for movements between the braincase and the dermal bones of the skull roof. Metakinesis is defined as a rotational movement between the braincase and the dermal skull roof about the metakinetic axis running transversely through the paroccipital processes. This movement manifests itself most conspicuously as a displacement between the supraoccipital and parietal bones, potentially also involving adjacent elements of the dermal skull roof. According to the quadric-crank model (Frazzetta, 1962), the parietal bone is rotated downward during mouth opening (coupled to a dorsal extension of the snout, i.e. mesokinesis). Metakinesis may provide some stabilisation in the amphikinetic skull (Frazzetta, 1986), but apart from this, no hypothesis has been put forward that highlights its functional or adaptive significance. To overstate the case, metakinesis is still somewhat of a myth: although some authors considered it to be a general and widespread pattern among Squamata (Arnold, 1998; Frazzetta, 1962; Iordansky, 2011), others argued that its existence has never been experimentally proven (Johnston, 2010; Metzger, 2002; Schwenk, 2000; Starck, 1979). According to Metzger (2002), the 'presence of metakinesis is essentially unconfirmed for all lepidosaurs and its anatomical basis is unclear'. The anatomy of the metakinetic joint is intricate. One of the most detailed descriptions of the joint was given for *Varanus* by Frazzetta (1962). He argued that the actual joint was formed by the processus ascendens tecti synotici (PATS), a rod-shaped process of the chondrocranium that originates from the anterior margin of the supraoccipital bone and inserts in a ventral depression of the parietal bone. According to Frazzetta, this joint permits some sliding movement of the PATS against the parietal bone. Later works showed that the histological nature of the metakinetic joint may vary strongly between taxa or even within the same genus (Condon, 1998; Rieppel, 1978a). Although data on the histological nature of the metakinetic joint remain sparse (Metzger, 2002; Schwenk, 2000), arguably the main reason why metakinesis remains to be poorly understood is that experimental studies have so far been unable to prove the nature and magnitude of metakinetic movements (Metzger, 2002).

Cranial kinesis is probably more likely to appear in small lizard species or juveniles of larger species. However, technical limitations of experimental procedures such as cineradiography or electromyography complicate investigation of feeding kinematics in small species. Thus, available data on lizard cranial kinesis are biased towards larger species, with little to no data so far available for very small or miniaturised species. Miniaturisation over evolutionary scales can lead to extensive remodelling of the skull (Gans, 1974). In squamates this may involve skull bone reduction, including the loss of the upper temporal arcade (Rieppel, 1984a,b, 1993). Furthermore, we hypothesise that miniaturisation can cause a reduced ossification of dermal elements of the skull owing to paedomorphosis, which could, in some taxa, lead to a higher mobility in the skull. Thus, data on cranial kinesis are badly needed for miniaturised squamates. To mitigate this lack of data, the present study on *Ablepharus kitaibelii* combines a thorough morphological investigation with experimental data on feeding kinematics and bite force, and a novel method of studying skull manipulations using microscopic 3D imaging. *Ablepharus kitaibelii* is one of the smallest lizards in the world, with an average head length of less than 7 mm (Ljubisavljević et al., 2002; Yildirim et al., 2017). Some data for *Ablepharus* skull morphology have previously been published. Haas (1935) made a detailed histological study of the skull based on transverse sections. Fuhn (1969) provided some data on osteology, and recently a detailed comparative study on the osteology of three *Ablepharus* species was published (Yildirim et al., 2017).

The present study on *A. kitaibelii* had three main aims. First, to provide a detailed description of the cranial architecture, including osteology, histology of cranial joints and analysis of cranial muscles. In particular, histological data on cranial joints are especially lacking for Scincidae (Payne et al., 2011). Second, to provide experimental data based on high-speed cinematography, bite force measurements and skull manipulations. So far, no experimental evidence has been advanced for the occurrence of mesokinesis and metakinesis in Scincidae (Metzger, 2002), whereas a study on *Corucia zebrata* and *Tiliqua scincoides* has shown that both mesokinesis and metakinesis are absent in these two species (Herrel et al., 1998). We measured mesokinetic movements during prey capture, processing and intraoral transport based on high-speed videos, and also studied the magnitude of intracranial movements during skull manipulations using microscopic X-ray computed tomography. And third, to formulate, using these data, an extended functional model for lizard amphikinesis with a special focus on the possible functional advantages of metakinetic movements. This model should be seen as a working hypothesis that can be tested in future studies on other small or miniaturised squamates.

MATERIALS AND METHODS

Terminology

In the present work we follow the terminology introduced by Versluys (1912, 1936) and later expanded by Frazzetta (1962). The skull is divided into an occipital segment (bony braincase), a maxillary segment (rest of the skull) and the lower jaws (mandibles). The maxillary segment includes five subunits: (i) muzzle unit, (ii) parietal unit, and the paired (iii) basal, (iv) epipterygoid and (v) quadrate units (muzzle unit plus basal units are equivalent to the palatomaxillary segment described by Smith, 1982). Metakinesis is defined as rotation movement between the braincase (occipital segment) and the skull roof (parietal unit) about the metakinetic axis. Mesokinesis is defined as movement between the muzzle unit and the parietal unit at the frontal–parietal suture. Streptostyly is defined as rotation of the quadrate around its dorsal articulation. Amphikinesis is combined meta- and mesokinesis (Frazzetta, 1962; Versluys, 1912, 1936). Hypokinesis, which refers to the flexion and extension of the palate around a transverse axis during mesokinesis (see also flexipalatality; Iordansky, 2011), will be discussed as part of mesokinetic movements instead of being treated as a distinct form of cranial kinesis (Metzger, 2002). Terminology of cranial muscles mostly follows Nash and Tanner (1970). For description of the gape cycles, we followed the terminology of Bramble and Wake (1985) and Schwenk (2000).

Animals

A total of 28 adult *Ablepharus kitaibelii* (Bibron and Bory de Saint-Vincent 1833) individuals were used in this study. The individuals were collected from Pancharevo, near Sofia (FN91), Bosnek Village (FN70) and Bezden Village (FN75), Bulgaria, caught under permit numbers 411/14.07.2011, 520/23.04.2013 and 656/08.12.2015 of the Ministry of Environment and Water, Bulgaria. All experiments were conducted in accordance with national animal welfare regulations.

High-speed cinematography

High-speed video recordings of feeding (food uptake, processing/manipulation and intraoral transport) of 12 adult specimens of *A. kitaibelii* were accomplished in a filming aquarium (50×30×30 cm) with a reference scale grid for calibration. During experiments, animals were fed with mealworms (*Tenebrio molitor* larvae) of equal size (length 1.5–2 cm; thickness 1.5–2 mm). Videos were recorded using a Photron FASTCAM 1024PCI high-speed camera (Photron, San Diego, CA, USA) and accompanying control software (Photron FASTCAM Viewer, v3600_64bit). The camera was equipped with a Nikon AF D 24-85/2.8-4IF Macro objective (Nikon Corporation, Tokyo, Japan). Illumination of the film set was created via usage of two Dedocool lights (Dedo Weigert Film GmbH, Munich, Germany). The majority of videos were recorded at 1000 frames s^{-1}, although some videos were made at 500 frames s^{-1}. The animals were consistently filmed in lateral view while feeding on mealworms. In total, more than 100 feeding events were captured, but the majority of videos did not show the head in an acceptable lateral orientation relative to the camera. Thus, the best 22 video sequences were chosen, resulting in eight recordings of food uptake (from eight individuals), 18 processing/manipulation cycles (from six individuals) and 15 intraoral transport cycles (from five individuals).

Video sequences were analysed with a custom motion tracking program (designed by C. Beisser and P. Lemell; programmed by C. Beisser) developed in MATLAB R2015b (MathWorks, Inc., Natick, MA, USA), which uses predictive algorithms based on a digitising software that was implemented in MATLAB by Hedrick (2008). Further analyses were performed with custom MATLAB scripts built in MATLAB R2015b. All analyses were done for three different feeding phases: (i) food uptake, defined as the initial process of grabbing a food item, followed by (ii) processing/manipulation cycles, defined as feeding cycles where the food item is manipulated by biting and lingual movements and not yet completely inside the oral cavity, and finally (iii) intraoral transport, which is defined as transport cycles inside the oral cavity, starting when the food item is completely inside the oral cavity and ending directly prior to pharyngeal packing (note that late intraoral transport cycles and pharnyngeal packing may blend in some cases). Regarding food uptake, one gape cycle per specimen was analysed; for processing/manipulation and intraoral transport, two to three gape cycles per individual were analysed. The *x*–*y* coordinates of the rostral tip of upper and lower jaw were tracked frame-by-frame to obtain information about the gape cycle. Based on the displacements, following kinematic variables were determined: (i) duration of gape cycle, (ii) duration of slow opening, fast opening, fast closing and slow closing power stroke phases, and (iii) mean and maximum velocities of opening and closing jaw movements. Furthermore, gape angle and mesokinetic angle were measured from still frames at the start of mouth opening, maximum gape and at the end of the gape cycle, in order to evaluate the maximum gape angle and the presence of mesokinesis. Two independent observers conducted analysis of mesokinetic angles. Although data presented in the paper are from observer 1, measurements conducted by observer 2 were highly comparable, and showed only minor deviations not affecting the general interpretation of mesokinetic movements.

Bite force measurements

Bite forces were measured for 11 adult specimens using an isometric Kistler force transducer (type 9203, range ±500 N; Kistler, Zurich, Switzerland) mounted on a purpose-built holder and connected to a Kistler charge amplifier (type 5995A, Kistler; see Herrel et al., 1999 for a more detailed description of the setup). As animals were reluctant to bite initially, the jaws were opened gently using flat-tipped tweezers. A thin layer of cloth tape was wrapped around the bite plates to provide better grip. Once the bite plates were placed between the jaws of the animal, however, prolonged and repeated biting resulted. The place of application of bite forces was standardised for all animals and gape angle was also standardised at 50 deg. Although bite force experiments on lizards are often performed at smaller gape angles, the large gape angle in *A. kitaibelii* was necessary because of the minute size of the animals compared with the testing device. Measurements were repeated five times for each animal and the maximal value obtained was considered to be the maximal bite force for that individual. In addition to measuring bite forces, we also measured snout–vent length, tail length, head length, head width, head depth and lower jaw length for each individual using digital callipers (Mitutoyo). Body mass was measured using an electronic balance (My Weight DuraScale D2 300). Morphometric and bite force data were $\log_{10}$ transformed before analysis. We ran a MANOVA to test for overall differences in head and body dimensions coupled to subsequent univariate ANOVAs. Differences between sexes in bite force were tested using a univariate ANOVA. To explore which variables best predicted variation in bite force, we ran a stepwise multiple regression with the morphometric data as predictors and bite force as our dependent variable. Finally, bivariate correlations were run between head dimensions and bite force. Bite forces in *A. kitaibelii* were compared with bite forces for other scincid lizards biting at a 30 deg gape angle. Species used for comparison included *Acontias percevali*, *Eumeces laticeps*, *Sphenops sepsoides*, *Chalcides ocellatus*, *Scincus scincus*, *Ctenotes uber*, *Cyclodomorphus michaeli*, *Eulamprus heathwoli*, *Lerista edwardsi*, *Morethia butleri*, *Tiliqua multifasciata*, *Tiliqua occipitalis*, *Tiliqua rugosa* and *Tiliqua scincoides* (data from previous studies provided by A.H.).

Skull manipulations

Four *A. kitaibelii* specimens (two adult males, two adult females) were euthanised with diethyl ether for 10–15 min. One male specimen was immediately fixed in 4% formaldehyde with closed mouth. For the three remaining specimens, the mouth was carefully opened by depressing the mandible with one hand while the other hand stabilized the neck of the specimen. Mouth opening was conducted until the person that carried out manipulations perceived a mechanical resistance, which was at a gape angle of approximately 60 deg. Subsequently, the opened mouth was filled with cotton to fix the mouth position for subsequent preparation steps. The three 'open mouth' specimens were then fixed in 4% formaldehyde for preservation. After fixation, specimens were stored in 70% ethanol.

Micro computed tomography image acquisition

Four specimens were subject to micro computed tomography (microCT) analysis: one specimen with closed mouth (male) and three specimens with opened mouth (one male, two females). Specimens were mounted in plastic tubes and scanned using a Scanco µCT35 (SCANCO Medical AG, Brüttisellen, CH) at 70 kVp (peak kilovoltage) and 114 µA current. The specimen with closed mouth was scanned at an isotropic voxel resolution of 3.5 µm [field of view (FOV)=7.2 mm]. The specimens with opened mouth were scanned with isotropic voxel resolutions of either 6 or 12 µm (FOV=12.3 mm). For reconstruction of cranial muscles, the specimen with the closed mouth (male) and one open mouth specimen (male) were dehydrated to absolute ethanol, stained with 1% elemental iodine in ethanol for 7 days, washed in absolute ethanol, and scanned with an isotropic voxel resolution of 7 µm.

Journal of Experimental Biology (2019) 222, jeb198291. doi:10.1242/jeb.198291

Image segmentation, measurement of muscle volumes and 3D visualisation of microCT scans

MicroCT image volumes were imported into the 3D software package Amira [FEI SAS, Mérignac, France (part of Thermo Fisher Scientific™)]. First, osteoderms (Fig. S1) were segmented and removed from image volumes using the Arithmetic tool to allow an undisturbed view on skull bones. For the iodine-stained specimen (closed mouth specimen), the two scans before and after staining were registered based on normalised mutual information. Subsequently, muscles involved in mouth opening and closing were segmented. Based on image segmentation, muscle volumes were measured. All image volumes (bones with osteoderms, bones without osteoderms, single muscles) were exported as separate volumes and visualised using Amira 6.4. and Drishti (Limaye, 2012).

Three-dimensional analysis of skull manipulations

MicroCT scans from four specimens (one with closed mouth, three with open mouth) were registered into the same coordinate system. First, the braincase was segmented for each scan. The occipital segment of the closed mouth specimen was aligned to the three anatomical planes. Next, the occipital segment of each of the three open mouth specimens was registered to the closed mouth specimen based on normalised mutual information, including an isometric scaling factor to correct for inter-subject size variation. Finally, the transformation matrix of the occipital segment was applied to the whole skull volume. The registered image volumes were used to set 13 anatomical landmarks in order to quantify skull kinetics (Fig. S2A). Kinetic angles were directly measured from landmark coordinates. In order to make the angle measurements comparable to studies based on high-speed video cinematography, angle measurements were projected to the sagittal plane (Fig. S2B). All angles measured relative to the vertical axis (quadrate rotation, epipterygoid rotation) have to be interpreted in relation to a stable occipital segment.

Histology

One *A. kitaibelii* specimen was fixed in Bouin's fixative for 5 months to ensure complete decalcification. It was embedded in paraffin wax, and sagittal sections were taken with a section thickness of 5 µm using a HM355S microtome (Thermo Fisher Scientific™, Waltham, MA, USA). Sections were stained with Haematoxylin & Eosin and imaged using a Zeiss Axio Imager Z1 (Carl Zeiss Microscopy GmbH, Oberkochen, Germany).

RESULTS

Cranial morphology

Description of skull bones based on microCT data

A detailed description of *A. kitaibelii* skull osteology based on cleared and stained specimens was published recently (Yildirim et al., 2017), thus we only quickly review the general characteristics of skull design relevant for cranial kinesis.

The head is covered by an armouring of bony osteoderms, except for parts of the frontal and parietal bones and parts of the snout region (Fig. S1). The occipital segment is formed by the basioccipital, the paired exoccipitals, the supraoccipital, the basisphenoid, the parasphenoid, and the paired prootics and opisthotics. The elements of the occipital segment are fused to a solid braincase (Fig. 1). The paroccipital processes are comparatively short. The basisphenoid shows two well-developed basipterygoid processes (Fig. 1C). The parietal unit consists of the unpaired parietal bone and the paired supratemporal, squamosal and postorbitofrontal bones. The parietal is a thin plate, showing two anterolateral shelfs that are overlapped by the frontal bone (Fig. 1F). The frontal–parietal suture (mesokinetic joint) is linear, lacking any kind of interdigitations (Fig. 1B). A complete upper temporal arcade is present. The supratemporal and squamosal bones are slender elements lying closely adjacent to the parietal. Thus, the upper temporal window is extremely narrowed and functionally absent (Fig. 1A,B). A comparatively large post-temporal fossa separates the parietal and supraoccipital bones (Fig. 1B). The quadrate bones dorsally articulate with the occipital segment and the supratemporal (Fig. 1A). The basal units are formed by paired pterygoids, ectopterygoids, palatines and jugals. The pterygoids bear no teeth and lack a medial process at the anterior end of the pterygoid notch (Fig. 1C). The jugals show a loose connection to the postorbitofrontal bones (Fig. 1A). The muzzle unit is formed by the unpaired frontal and the paired nasals, premaxillae, maxillae, septomaxillae, vomers, prefrontals and lacrimals (Fig. 1). The strut-like epipterygoid bones ventrally articulate with the pterygoids and dorsally do not contact the prootics (Fig. 1A). The paired mandibles are formed by the dentary, coronoid, splenial, angular, surangular, prearticular and articular. The retroarticular process is long and slender (Fig. 1A). The two rami of the mandibles show no bony fusion (Fig. 1D). Other ossifications of the skull include the columellae, orbitosphenoid bones, superciliary bones, hyoid apparatus and scleral rings.

The processus ascendens tecti synotici

The PATS is part of the chondrocranium, and it was entirely cartilaginous in all analysed specimens (N=5). It is a thin rod in the midsagittal plane, its origin is the anterior margin of the supraoccipital and it inserts in a ventral groove of the parietal. Thus, the PATS lies directly at the level of the presumed metakinetic joint, connecting the occipital segment with the parietal unit of the maxillary segment (Fig. 1B,E,F). In the closed mouth condition, the anterior tip of the PATS is in close contact with the parietal bone, to which it is connected by connective tissue (Fig. 2A).

Description of skull joints based on histology

Both the presumed mesokinetic joint between the frontal and parietal (Fig. 2C) and the putative metakinetic joint between the parietal and supraoccipital (Fig. 2B) are syndesmotic. The frontal and parietal are thin, plate-shaped bones and the frontal–parietal joint shows no interdigitations. Each of the quadrate bones has three joints. First, it forms the synovial jaw joint with the articular bone of the mandible (Fig. 2E). Second, it is connected to the quadrate ramus of the pterygoid by the quadratopterygoid ligament (Fig. 2E). Last, it is attached to the paroccipital process of the exoccipital and the supratemporal by a synchondrosis (Fig. 2D). The paired pterygoid bones possess five joints. Next to the quadratopterygoid ligament connection to the quadrate, they form the synovial basipterygoid–pterygoid joint with the basisphenoid (Fig. 2F), a synovial joint with the epipterygoid (Fig. 2G), and a syndesmotic joint with the palatine (Fig. 2H) and the ectopterygoid.

Description of cranial muscles based on microCT data

The description of cranial musculature is not exhaustive and only focuses on muscles relevant during mouth opening and closing, which are illustrated using microCT slices (Fig. 3) and 3D renderings (Figs S3 and S4). Concerning mouth opening, the m. depressor mandibulae (MDM) originates mainly from a fascia and partly also from the posterior part of the squamosal, and inserts at the retroarticular process of the mandible (Fig. S3A). The m. levator pterygoideus (MLPT) is a slender muscle originating via a tendon from the ventral surface of the parietal, and runs parallel to the epipterygoid and inserts at the pterygoid just posterior to the

Journal of Experimental Biology (2019) 222, jeb198291. doi:10.1242/jeb.198291

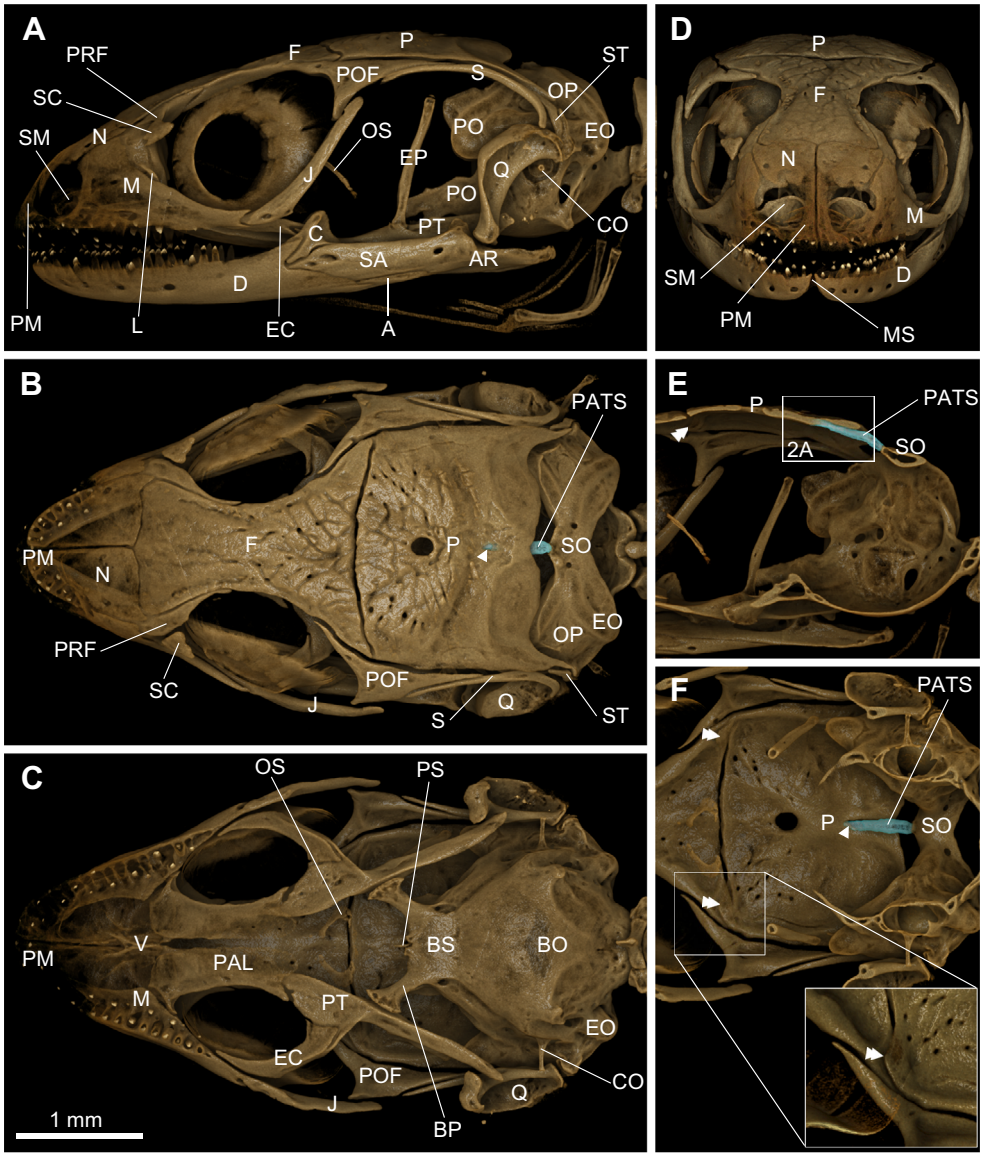

Fig. 1. Cranial osteology and the cartilaginous PATS in *Ablepharus kitaibelii* depicted based on volume renderings from a microCT image volume. (A) Lateral view. (B) Dorsal view. (C) Ventral view of the palate, with mandibles removed. (D) Cranial view. (E) Lateral view virtually cut close to the mid-sagittal plane. (F) Ventral view. The paired anterolateral shelfs of the parietal bone (double arrowheads) are overlapped by the frontal bone. Arrowheads indicate the distal tip of the PATS. A, angular; AR, articular; BO, basioccipital; BP, basipterygoid process; BS, basisphenoid; C, coronoid; CO, columella; D, dentary; EC, ectopterygoid; EO, exoccipital; EP, epipterygoid; F, frontal; J, jugal; L, lacrimal; M, maxilla; MS, mandibular symphysis; N, nasal; OP, opistothic; OS, orbitosphenoid; P, parietal; PATS, processus ascendens tecti synotici; PAL, palatine; PM, premaxilla; PO, proothic; POF, postorbitofrontal; PRF, prefrontal; PS, parasphenoid; PT, pterygoid; Q, quadrate; S, squamosal; SA, surangular; SC, superciliary; SM, septomaxilla; SO, supraoccipital; ST, supratemporal; V, vomer.

pterygoid–epipterygoid joint (Fig. 3C and Fig. S3B). The m. protractor pterygoideus (MPPT) is a well-developed muscle that originates from the anteroventral part of the prootic and inserts at the medial surface of the quadrate ramus of the pterygoid (Fig. 3B–E and Fig. S3B). The m. spinalis capitis (MSC) originates along the vertebrae and inserts along the posterior edge of the parietal (Fig. 3B and Fig. S3C). Concerning mouth closing, the m. adductor mandibulae externus (MAME) is by far the most voluminous muscle in the skull (Table S1). The largest number of MAME fibres originates from the ventral surface of the lateral portion of the parietal and the ventral surface of the postorbitofrontal, squamosal and supratemporal (Fig. 3A,C and Fig. S4A). Some fibres of the deep portions of the MAME also originate from the prootic (Fig. 3B). The MAME inserts at a large portion of the dorsomedial surface of the mandible between the coronoid and the quadrate–articular joint (Fig. S4A). Posterior to the MAME lies the m. adductor mandibulae posterior (MAMP), which originates at the quadrate bone and inserts at the mandible just anterior of the quadrate–articular joint (Fig. 3A and Fig. S4A). The m. pseudotemporalis lies deep to the MAME (Fig. 3B–D and Fig. S4B). It mainly originates from the anterior part of the prootics (some fibres originate from the epipterygoid and maybe also from the ventral surface of the parietal) and inserts at the coronoid and surangular (Fig. S4B). The m. pterygoideus is the second largest adductor muscle (Table S1) and originates mainly from the pterygoid and attaches to the angular, surangular, articular and retroarticular process (Fig. 3A–C,F and Fig. S4C).

Cranial kinesis during skull manipulations (depression of lower jaw)

Results of manipulations are summarised in Table 1. During skull manipulation, the mandible of freshly killed specimens was depressed while the neck of the specimens was stabilised, resulting in an average mouth gape angle increase of 58.2 deg. The mesokinetic angle measured 162.1 deg in the closed mouth state and on average 169.6 deg in the open mouth state. This means that the snout was dorsally extended by 7.5 deg around the mesokinetic axis. Mesokinetic extension was accompanied by a mean 2.6 deg change in the hypokinetic angle of the palate. The metakinetic angle measured 113.5 deg with closed mouth and 103.3 deg with open mouth, resulting in a difference of 10.2 deg. This change in metakinetic angle reflects the downward rotation of

Journal of Experimental Biology (2019) 222, jeb198291. doi:10.1242/jeb.198291

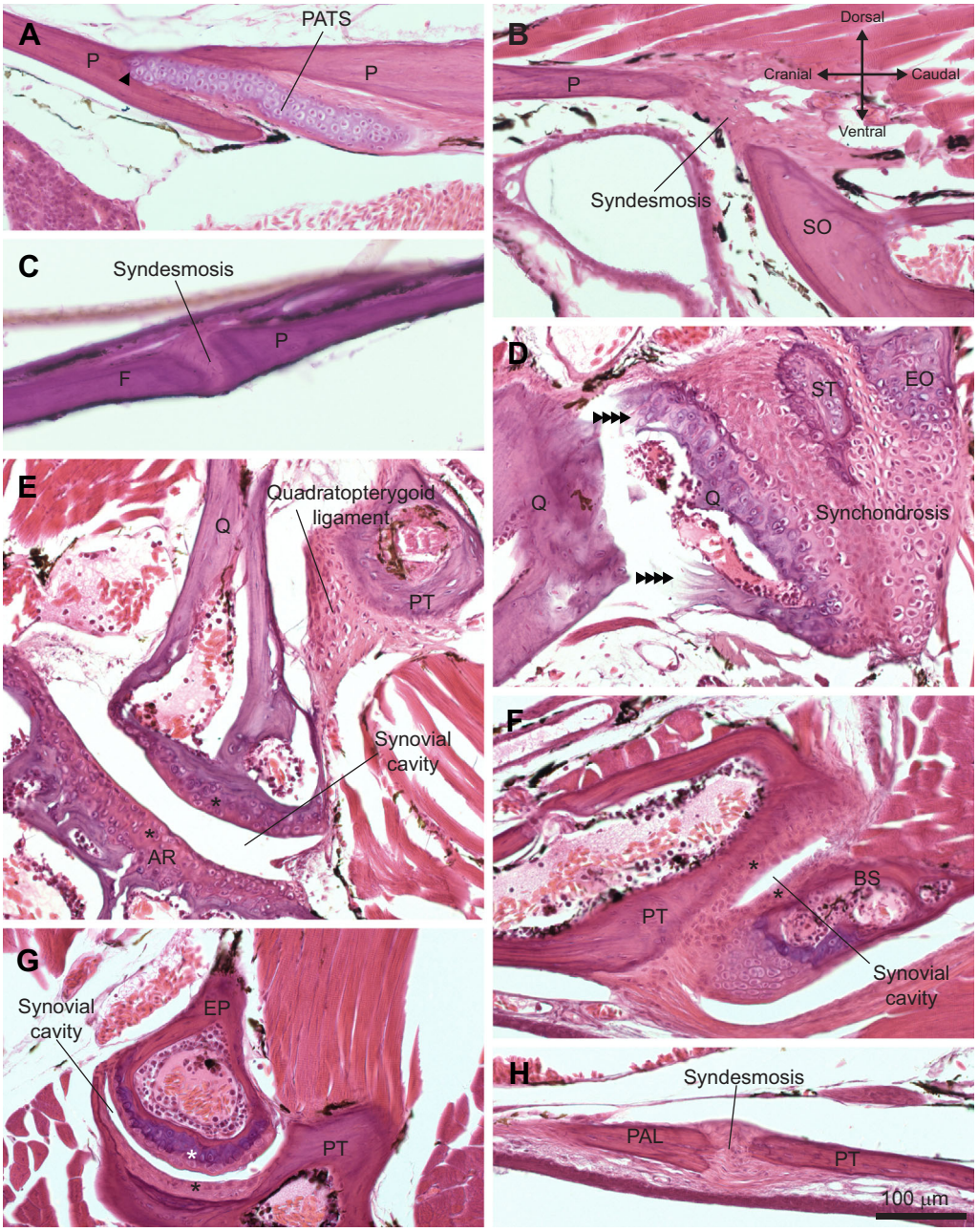

Fig. 2. Histology of cranial joints of *A. kitaibelii* depicted based on midsagittal and parasagittal sections. (A) Connection between the PATS and the parietal bone in the mid-sagittal plane. (B) Syndesmotic connection of the parietal and supraoccipital (part of the metakinetic joint). (C) Syndesmotic frontal–parietal suture (mesokinetic joint). (D) Synchondrotic joint between the quadrate and the supratemporal and exoccipital (paroccipital process). Multiple arrowheads indicate that the quadrate was disrupted as an artefact of histological sectioning. (E) Synovial jaw joint between quadrate and articular, and syndesmotic connection between quadrate and pterygoid by the quadratopterygoid ligament. (F) Synovial joint between the basipterygoid process of the basisphenoid and the pterygoid. (G) Synovial joint between pterygoid and epipterygoid. (H) Syndesmosis between pterygoid and palatine. Scale bar applies to all images. For abbreviations, see Fig. 1. *Articular cartilage.

the skull roof against the braincase about the metakinetic axis. The angle of the quadrate to the vertical axis was 41.0 deg with a closed mouth and 55.1 deg with an open mouth, confirming that streptostyly is possible with a quadrate rotation of 14.1 deg in the anterior direction. Finally, the angle of the epipterygoid was 13.9 deg with a closed mouth and 23.4 deg with an open mouth. This not only shows rotation of the epipterygoid by 9.5 deg, it also shows that a protraction of the pterygoid in respect of the occipital segment occurred. This is in line with the visual observation in microCT image volumes (Movie 1).

Feeding kinematics observed by high-speed cinematography

Kinematic variables for the gape cycles and measurements of mesokinesis are summarised in Table 2. Selected video frames and mean kinematic profiles are shown in Fig. 4.

Food uptake

Ablepharus kitaibelii detected the prey visually; on some occasions, tongue flicking with touching of the prey was observed. Feeding started with lifting of the body and bending the head ventrally. Afterwards, the prey was captured with the anterior teeth by pure jaw prehension. Usually, prey prehension was immediately followed by prey shaking (see Natchev et al., 2015). Mean gape cycle duration during food uptake was 100.7 ms. A slow open phase (SO) was detected in only 50% of the analysed videos. It was followed by a fast open phase (FO) with a mean duration of 42.8 ms and a mean opening velocity of 55.9 mm s^{-1}. A short plateau phase (maximum gape phase *sensu* Natchev et al., 2009) of 5–30 ms was followed by the fast close phase (FC) with a mean duration of 12.9 ms and a mean velocity of 102.9 mm s^{-1}. After touching the prey at the end of FC, a second closing phase was detected, which is defined as slow close–power stroke (SC–PS). During food uptake, the mean maximum gape

Journal of Experimental Biology (2019) 222, jeb198291. doi:10.1242/jeb.198291

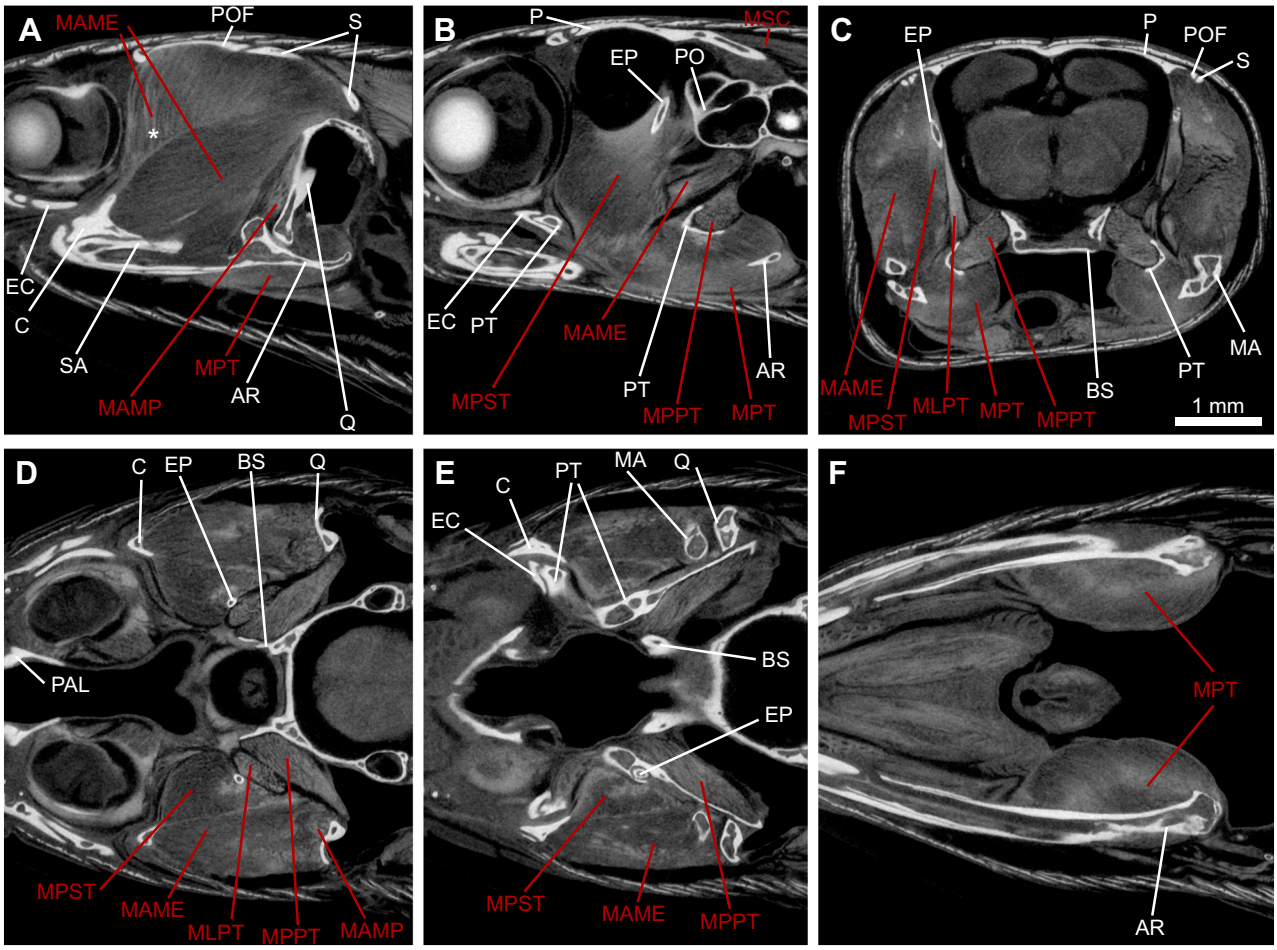

Fig. 3. Cranial musculature of *A. kitaibelii* depicted based on microCT sections from an iodine-stained specimen scanned with closed mouth. (A) Sagittal section through the m. adductor mandibulae externus (MAME), showing its pennation and the coronoid aponeurosis (*). (B) Sagittal section through the m. pseudotemporalis lying deep to the MAME, and the m. pterygoideus. (C) Transverse section at the position of the epipterygoids, showing the origin of the MAME at the ventral surface of different elements of the parietal unit. (D) Frontal section depicting jaw adductors and pterygoid-associated muscles at the height of the eye. (E) Frontal section taken slightly dorsal to the quadrate–articular joint (ventral to D), depicting the course of fibres of the m. protractor pterygoideus. (F) Frontal section taken ventral to the quadrate–articular joint (ventral to E), depicting the m. pterygoideus mass. Muscle abbreviations (depicted in red): MAME, m. adductor mandibulae externus; MAMP, m. adductor mandibulae posterior; MLPT, m. levator pterygoideus; MPPT, m. protractor pterygoideus; MPT, m. pterygoideus; MPST, m. pseudotemporalis; MSC, m. spinalis capitis. For bone abbreviations (depicted in white), see Fig. 1.

angle was 35.1 deg, while the largest measured maximum gape angle was 43.0 deg. Measurements of the mesokinetic angle at the frontal–parietal joint showed that dorsal extension of the muzzle unit occurs during mouth opening, while ventral flexion of the muzzle unit occurs during mouth closing. From the angle at the starting position, a mean increase of 3.9 deg was seen during maximum gape, while the highest measured mesokinetic extension angle during a food uptake sequence was 7.7 deg. At the end of FC, the angle was almost identical as at the start of the gape cycle (Table 2).

Processing/manipulation

After food uptake, some processing cycles were observed. Processing started with manipulating the prey with the lingual apparatus to orient it inside the oral cavity. Afterwards, a series of biting cycles took place, supported by lingual movements where the tongue moved underneath the prey during SO. Typical processing cycles did not involve intraoral transport. The mean gape cycle duration was approximately three times as long as during food uptake (323.1 ms). A clear SO was visible; FO and FC were again interrupted by a short plateau phase. In most recorded processing/manipulation cycles, a clear SC–PS was detected. Gape angles were similar to those during food uptake, but differences were found in the pattern of mesokinesis. We observed a mean mesokinetic extension of approximately 3.0 deg at maximum gape and a mean flexion of approximately 3.5 deg at the end of FC, but during SC–PS, a further flexion of approximately 2.9 deg could be measured, which was also clearly observable in the video sequences.

Intraoral transport

During this phase, the prey was positioned completely inside the oral cavity and shifted backwards mainly by lingual retraction. The tongue formed a triangular shape around the end of the prey and pushed the prey towards the oesophagus. Gape cycle duration was similar to processing cycles: an SO was always present, and FO and FC were again interrupted by plateau phase. An SC–PS phase was missing or integrated within the normal closing phase. Mean and maximal velocities of FO and FC were slower than during processing cycles. Mesokinetic movements were again observed with 2.3 deg extension and 3.7 deg flexion on average.

Bite force measurements

Ablepharus kitaibelii showed slight sexual dimorphism, with head width ($F_{1,9}$=8.07, P=0.019) and body mass ($F_{1,9}$=13.66; P=0.005)

Journal of Experimental Biology (2019) 222, jeb198291. doi:10.1242/jeb.198291

Table 1. Measurements of kinetic angles based on skull manipulations and microCT imaging in *Ablepharus kitaibelii*

	Closed mouth (*N*=1) (deg)	Open mouth (*N*=3; mean±s.d.) (deg)	Angle difference during jaw opening (deg)
Gape angle	4.22	62.42±3.54	+58.20
Mesokinetic angle	162.16	169.64±1.63	+7.49
Metakinetic angle	113.45	103.26±4.57	−10.19
Quadrate angle	40.98	55.13±3.40	+14.14
Epipterygoid angle	13.86	23.39±3.09	+9.53
Hypokinetic angle	173.44	176.03±4.31	+2.59

Measurements were taken from one specimen with a closed mouth (male) and three specimens with an open mouth (one male, two females). For explanation of measured angles, see Fig. S2B.

being larger in males compared with females (Table 3). Bite forces were also significantly different between sexes, with males biting significantly harder than females ($F_{1,9}$=8.48, P=0.017; Table 3). A stepwise multiple regression extracted head width as the best predictor of bite force across individuals (R^2=0.72, P<0.001; Fig. 5A). Other head dimensions were also correlated with bite force (all P<0.05) but were generally poorer predictors of the overall variation in bite force. When compared with a broad sample of other scincid lizards, *A. kitaibelii* showed lower bite forces compared with larger scincids, with presumably less kinetic skulls and biting at lower gape angles (Fig. 5B).

DISCUSSION

Observations on *A. kitaibelii* cranial morphology

Our study provides substantial morphological data concerning skull osteology, head muscles and the histological nature of the skull joints of the miniaturised scincid *A. kitaibelii*. In particular, histological data on skull joints have so far been entirely missing for Scincidae (Payne et al., 2011). The general osteology and myology reveals a similar musculo-skeletal morphology compared with previous studies on *Ablepharus* and other members of the Scincidae (Caputo, 2004; Haas, 1935; Nash and Tanner, 1970; Paluh and Bauer, 2017; Wineski and Gans, 1984; Yildirim et al., 2017). Skull shape is similar to that of other small scincids (Caputo, 2004; Paluh and Bauer, 2017). The histological nature of joints in the *A. kitaibelii* skull relevant for cranial kinesis is similar compared with that of other highly kinetic squamates such as geckos (Mezzasalma et al., 2014; Payne et al., 2011).

Results of our morphological analysis indicate a clear potential for cranial kinesis in the *A. kitaibelii* skull. This includes numerous features that have been previously assumed to represent morphological correlates of cranial kinesis (Metzger, 2002). Morphological indications for mesokinesis include: (i) a linear syndesmotic frontal–parietal joint lacking any kind of interdigitation (Fig. 1B), (ii) the narrowing of the upper temporal window (Fig. 1B), (iii) a flexible connection between the jugal and postorbitofrontal bones (Fig. 1A), (iv) a loose syndesmotic connection between the pterygoid and palatine, allowing for hypokinesis (Fig. 2H), (v) a synovial basipterygoid joint (Fig. 2F), (vi) absence of a medial pterygoid process that would restrict movement at the basipterygoid joint (Fig. 1C) and (vii) a loose connection between the epipterygoid and parietal and prootic bones (Fig. 1A). Indications for metakinesis include: (i) a large syndesmotic post-temporal fossa between the parietal bone and the supraoccipital bone (Figs 1B and 2B), (ii) a cartilaginous PATS that can be flexed ventrally during mouth opening (Figs 1B,E,F and 2A), (iii) the two well-pronounced anterolateral shelves of the parietal bone that are overlapped by the frontal bone, causing a depression of the parietal unit once the muzzle is elevated (Fig. 1F), and (iv) the flexible synchondrotic connection between the lateral posterior tips of the parietal unit and the occipital segment (Fig. 2D). Indications for streptostyly include: (i) the synchondrotic connection between the quadrate bones and the occipital segment and supratemporal (Fig. 2D), and (ii) the connection between the quadrate and pterygoid bones by the quadratopterygoid ligament (Fig. 2E). Analysis of head musculature also supported the general hypothesis of a highly kinetic skull. The m. protractor pterygoideus, which is considered as a main driver for mesokinetic movement, is well developed (Fig. 3D,E and Fig. S3B).

Evaluations of manipulated specimens corroborated the hypothesis of a highly kinetic skull. Three-dimensional microCT

Table 2. Kinematic variables of *A. kitaibelii* feeding on mealworms during food uptake, processing/manipulation and intraoral transport

	Food uptake (*N*=8)	Processing/manipulation (*N*=18)	Intraoral transport (*N*=15)
Gape cycle duration (ms)	100.7±32.1	323.1±206.1	332.0±164.6
SO duration (ms)	31.8±18.2	161.9±180.0	179.1±115.9
FO duration (ms)	42.8±11.5	42.7±51.5	51.1±20.9
FO mean velocity (mm s^{-1})	55.9±25.2	34.0±26.7	21.6±9.0
FO max. velocity (mm s^{-1})	128.4±30.4	62.3±32.3	45.4±11.8
Plateau duration (ms)	18.5±14.4	10.8±6.4 (*N*=15)	18.8±17.6
FC duration (ms)	12.9±6.7	43.2±31.8	93.1±77.9
FC mean velocity (mm s^{-1})	102.9±38.9	39.7±34.1	27.0±11.6
FC max. velocity (mm s^{-1})	149.6±41.3	76.3±32.3	58.2±14.6
SC–PS duration (ms)	28.2±6.0 (*N*=5)	44.4±30.1 (*N*=14)	n.a.
Max. gape angle (deg)	35.1±4.1	34.6±4.2	33.2±4.5
Mesokinetic extension (deg) (start–max. gape)	+3.89±2.70	+2.97±2.96	+2.31±3.21
Mesokinetic flexion (deg) (max. gape–end of FC)	−3.88±2.14	−3.48±2.63	−3.74±2.83
Mesokinetic flexion power stroke (deg) (max. gape–end of SC–PS)	n.a.	−6.36±1.99 (*N*=14)	n.a.

Upper part of the table shows kinematic variables of the gape cycle, lower part shows mesokinetic movements. Number of video recordings is given in header (*N*; values that differ are indicated within the table); max. velocity is an average value of the five highest velocities during the respective phase. FC, fast closing; FO, fast opening; SC–PS, slow closing–power stroke; SO, slow opening. Data are means±s.d.

Journal of Experimental Biology (2019) 222, jeb198291. doi:10.1242/jeb.198291

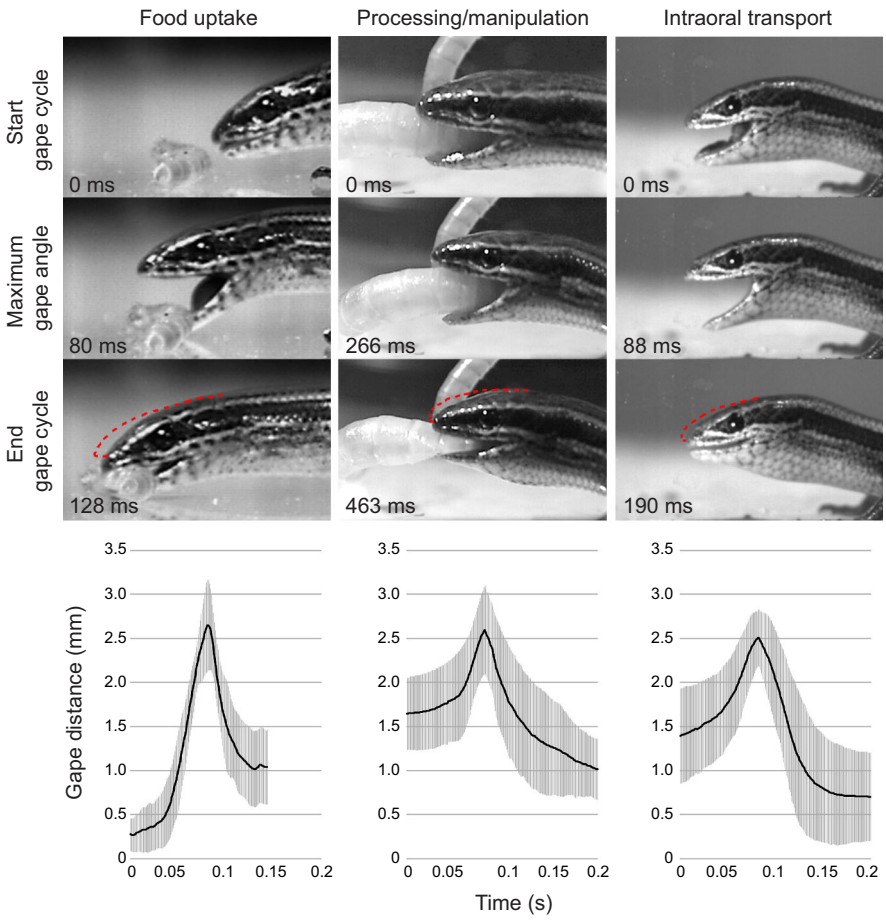

Fig. 4. Feeding kinematics of food uptake, processing/manipulation and intraoral transport in *A. kitaibelii* feeding on mealworms. Still frames from high-speed recordings show a lateral view of the three feeding phases at three selected time points, which are the beginning of the gape cycle, maximum gape angle and the end of the gape cycle. Red dashed lines indicate the head contour during maximum gape, showing that mesokinetic extension occurs during all three feeding phases. Bottom row shows mean gape cycle kinematics for food uptake (n=8 analysed sequences), processing/manipulation (n=18) and intraoral transport (n=15). Note that the intraoral transport phase may blend with early pharyngeal packing. Further note that the selected sequence of processing/manipulation shows an exceptionally long slow open phase.

images showed average angular changes of 10.2 deg for metakinesis, 7.5 deg for mesokinesis and 14.1 deg for streptostyly (Table 1). Previous authors noted that morphological analyses and skull manipulations could only indicate the potential of cranial kinesis, while experimental techniques are needed to evidence kinesis in the living animal (Hofer, 1960; Iordansky, 2011; Metzger, 2002). We agree with this conclusion, but we think that our new skull manipulation approach including 3D imaging, as first described in the present paper, adds a new dimension to the investigation of cranial kinesis in vertebrate skulls. It allows for accurate quantification of even small and intricate changes in angles and distances in the intact head (including musculature, connective tissues and skin) of freshly killed specimens. Furthermore, in our manipulation approach, some types of kinesis such as metakinesis are revealed passively as a consequence of mouth opening and not by active pushing or pulling on the parietal units (as during conventional manipulations of ligamentous specimens). It has to be noted, however, that gape angles generated during skull manipulations were larger compared with those observed during feeding behaviour. Thus, changes in kinetic angles are presumably smaller in the living animal compared with measurements from skull manipulations, as seen in mesokinetic extension, which was 3.9 deg during mouth opening during prey capture compared with 7.5 deg in skull manipulations. Despite quantitative differences, we expect the general observed pattern from skull manipulations as representative for living animals, owing to the observed morphological links.

Table 3. Summary table describing morphology and bite force of the individual *A. kitaibelii* used for the bite force measurements

	Males (N=6)	Females (N=5)
Snout–vent length (mm)	41.67±2.10	41.74±1.34
Mass (g)	**1.03±0.10**	**0.76±0.13**
Tail length (mm)	43.27±8.91	37.25±25.08
Head length (mm)	6.68±0.47	6.27±0.39
Head width (mm)	**3.82±0.21**	**3.45±0.23**
Head depth (mm)	2.70±0.19	2.47±0.19
Lower jaw length (mm)	5.94±0.77	5.78±0.37
Bite force (N)	**0.39±0.16**	**0.21±0.04**

Data are means±s.d. Bold values illustrate significant differences between sexes (P<0.05).

Experimental data from living animals

Before the present study, no scincomorphs had been experimentally shown to exhibit any type of cranial kinesis other than streptostyly (Metzger, 2002), and studies on *Corucia zebrata* and *Tiliqua scincoides* showed a lack of mesokinesis and metakinesis (Herrel et al., 1998). However, several morphological studies indicated the potential for cranial kinesis for several members of the group, e.g. for the genus *Trachylepis* (Paluh and Bauer, 2017). High-speed analysis of *A. kitaibelii* gape cycles confirmed the hypothesis of a kinetic skull. During all investigated feeding phases, mesokinesis could be detected. Dorsal extension of the muzzle unit was seen during mouth opening, while ventral flexion of the snout was detected during mouth closing (Fig. 4, Table 2). In addition, the slow close–power stroke phase during processing/manipulation showed even stronger flexion of the snout (Table 2). Although these data unambiguously indicate the presence of mesokinesis, the presence of metakinesis cannot be experimentally proven using high-speed cinematography.

Journal of Experimental Biology (2019) 222, jeb198291. doi:10.1242/jeb.198291

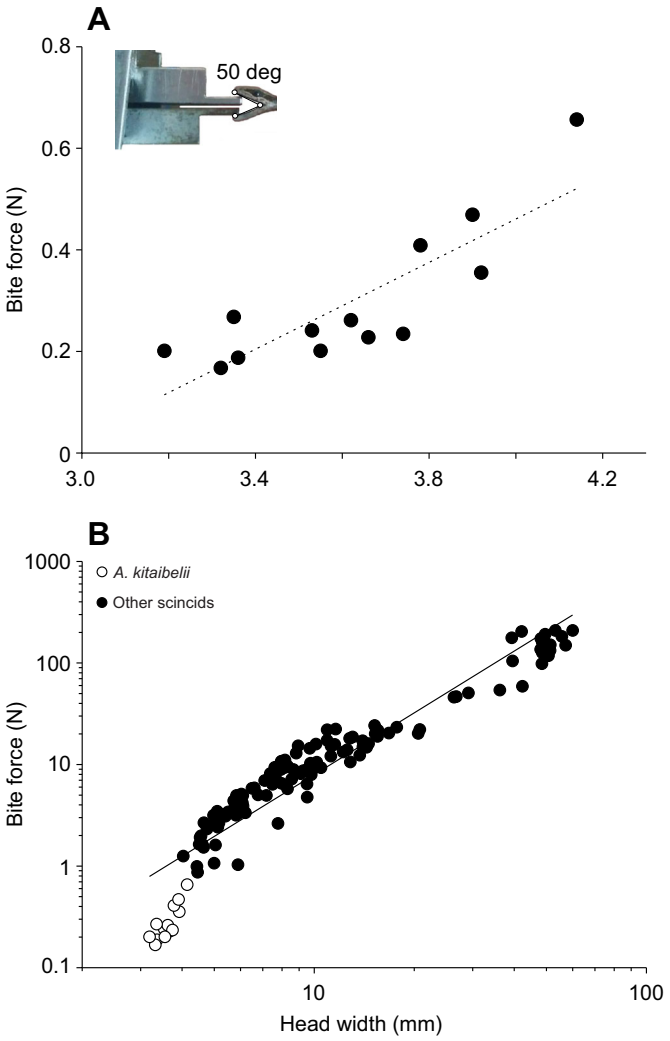

Fig. 5. Plots of bite force versus head width in *A. kitaibelii* compared with other scincids. (A) Bite forces increased with head width as would be expected. (B) Compared with larger scincid lizards biting at a gape angle of 30 deg, bite force was relatively smaller in *A. kitaibelii* biting at a large gape angle (50 deg). However, despite the large gape, *A. kitaibelii* was able to maintain bite force at relatively high levels, possibly owing to reduction in fibre stretch permitted by the observed cranial kinesis.

Nevertheless, the presence of metakinesis seems very likely, as frontal and parietal bones show a functional link at the mesokinetic joint (Fig. 1F) that automatically rotates the parietal downward at a certain point of mesokinetic extension. Generally, kinematic measurements showed that feeding movements in *A. kitaibelii* are fast. Especially during food uptake, duration of the fast opening and fast closing phases are short, which is accomplished by high fast opening and fast closing velocities (Table 2). Bite force relative to head width was smaller in *A. kitaibelii* compared with bite forces measured for larger scincid species. This observation is plausible given that (i) *A. kitaibelii* was biting at larger gape and (ii) it has a kinetic skull, whereas larger scincids presumably show less potential for mesokinesis and metakinesis, and it was previously shown that having a kinetic skull results in a reduced bite force (Herrel et al., 2007). The comparative interpretation of presented data, however, is somewhat limited by the fact that *A. kitaibelii* was biting at a larger gape angle than larger species used for comparison, and bite forces of *A. kitaibelii* will be higher when biting at 30 deg gape angle. This could be addressed in a future study using a smaller testing device. However, *A. kitaibelii* showed prolonged and reasonably hard biting even at a gape angle of 50 deg.

An extended model for squamate amphikinesis

Based on the present data, we here formulate an extended hypothesis for lizard amphikinesis based on the skull of *A. kitaibelii* (graphically summarized in Fig. 6). Our model is founded on the fact that, upon manual manipulation involving the depression of the mandible, mesokinetic, metakinetic and streptostylic movements were observed. It thus is clearly a model of coupled kinetics, where mouth opening is causal for several other coupled processes in the skull. Movements observed during skull manipulations are in accordance with Frazzetta's quadric crank model: the parietal unit is rotated downward against the braincase about the metakinetic axis (metakinesis), while the muzzle unit rotates upwards (mesokinesis) and the quadrate swings forward (streptostyly). This results in a flattened skull roof and an elevated snout, while the palate is protracted and elevated (Movie 1).

Mouth opening (Fig. 6E) starts with depression of the mandible (1). During our skull manipulations, this was done by hand, whereas in the living animal depression is accomplished by action of the MDM (Fig. S3A). (2) Quadrate rotation occurs as a direct consequence of depression of the mandible. (3) Quadrate rotation drives the protraction of the basal unit, owing to the connection of the quadrate and pterygoid by the quadratopterygoid ligament (Fig. 2E). In the living animal, protraction of the basal unit may be actively reinforced by action of the MPPT. (4) Protraction of the basal unit causes mesokinetic extension of the muzzle unit and rotation of the epipterygoid bones. (5) Mesokinetic extension of the muzzle unit initiates metakinetic movement. Once the frontal bone is increasingly dorsally extended, it will push the two underlying anterolateral shelves of the parietal bone (Fig. 1F) downward, thus depressing the anterior part of the parietal bone. This results in a downward rotation of the parietal unit around the metakinetic axis. With ongoing mandible depression and larger gape angles, downward rotation of the parietal unit is reinforced by ventral pulling of the parietal unit via the MAME, which connects the mandible to the ventral surface of the parietal, postorbitofrontal, squamosal and supratemporal. Downward rotation of the parietal unit might be guided and controlled by the PATS, which to some extent might restrict metakinetic movements and potentially helps to protect the brain.

Mouth closing (Fig. 6F) involves the action of several muscles. The MAME, MPST and MPT close the mandible (7), while the basal unit (pterygoid) is retracted (8). (9) Retraction of the pterygoid may cause a ventral flexion at the mesokinetic joint beyond the resting position of the muzzle unit, as observed in processing cycles during the slow close–power stroke phase (Table 2). (10) Finally, the parietal unit is brought to its resting position. Again we hypothesize that the PATS fulfils an important function in guiding movements of the parietal unit during mouth closing. It may help to stabilise the resting position of the skull roof after mouth closure. Hypothetically, the PATS, which is ventrally bent during mouth opening, may even contribute to actively push back the parietal unit to its resting position. However, based on the current data, we think that it is too small to store sufficient elastic energy to fulfil this function.

New elements in the presented model for squamate amphikinesis

Skull manipulations showed that mesokinesis and metakinesis can be directly driven by depression of the mandible. The presented model must be considered as an extension of Frazzetta's (1962) model of the amphikinetic skull, including some new hypothesis on the involved morphological features and functional links and expanding

Journal of Experimental Biology (2019) 222, jeb198291. doi:10.1242/jeb.198291

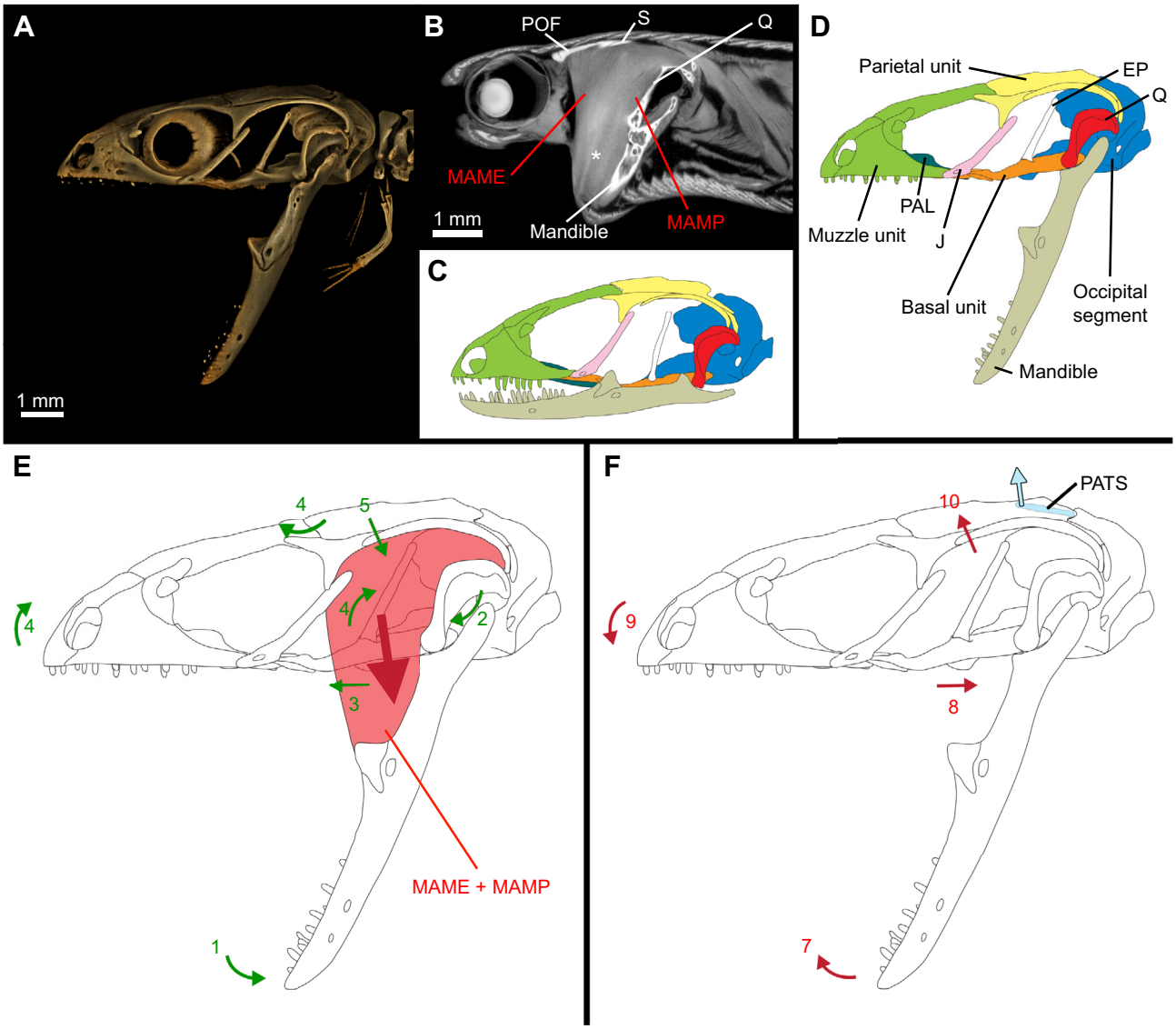

Fig. 6. A functional model for cranial kinesis of *A. kitaibelii* based on artificial skull manipulations and microCT imaging. (A) Volume rendering of a microCT scan of a specimen with opened mouth. Skull manipulation, i.e. depression of the lower jaw, was performed right after the animal was euthanized. (B) Sagittal microCT section, showing the mandible adductors. Note that at approximately 60 deg gape, the course of the MAME fibres is almost vertical. (C) Schematic drawing of the *A. kitaibelii* skull with closed mouth. (D) Schematic drawing of the *A. kitaibelii* skull with artificially opened mouth. Note that the jugal and palatine bones show distinct movability with respect to the basal, parietal and muzzle unit, and thus should be seen as separate entities in the kinetic mechanism. (E) Our hypothetical functional model for *A. kitaibelii* amphikinesis and streptostyly during mouth opening. Depression of the mandible (1) causes rotation of the quadrate, i.e. streptostyly (2). Quadrate rotation protracts the basal units (3). This protraction causes both a lifting of the muzzle unit (mesokinetic extension) and rotation of the epipterygoid (4). Lifting of the muzzle unit initiates depression of the anterior margin of the parietal bone, as the posterior edge of the frontal pushes the paired anterolateral shelfs of the parietal bone (Fig. 3C) downward, resulting in metakinesis (5). In addition, ongoing depression of the mandible at large gape angles might create a ventral pull on the MAME, resulting in a reinforced ventral depression of the parietal unit (reinforced metakinesis). (F) Our hypothetical model for *A. kitaibelii* amphikinesis and streptostyly during mouth closing. Action of the jaw adductor muscles causes an elevation of the mandible (7) and retraction of the basal unit (8). Ventral flexion of the muzzle unit happens as consequence of basal unit retraction (9). Finally, the parietal unit is brought back into its dorsal resting position, which may involve action of the m. spinalis capitis (not shown). The cartilaginous PATS helps to stabilize the resting position of the parietal bone (10). For abbreviations, see Figs 1 and 4. *Coronoid aponeurosis.

Frazzetta's model in three critical aspects that are important for metakinesis. (i) We hypothesize that the two anterolateral shelves of the parietal bone are critical for parietal unit depression during snout elevation. This functional link is appealing, as it suggests that once the snout is elevated above a certain threshold, the posterolateral edges of the frontal bone will push the parietal bone downward thus causing a flattened skull roof as observed in the amphikinetic skull. Anterolateral shelves of the parietal bone have been reported for other squamates such as *Trachylepis* (Paluh and Bauer, 2017) and *Sphaerodactylus* (Daza et al., 2008), but so far they have not been discussed as a possible functional link in the kinetic skull mechanism. We hypothesise that they could be an indication of amphikinesis, which requires investigation of this trait across different lizard taxa. (ii) We hypothesise that metakinesis in the *A. kitaibelii* skull is not exclusively accomplished by mesokinetic extension of the muzzle unit and the above-described mechanism, but for large gape angles it is also reinforced by the MAME. We argue that despite a certain elasticity of the MAME and its aponeurosis, it passively transmits a

Journal of Experimental Biology (2019) 222, jeb198291. doi:10.1242/jeb.198291

ventral pull from the mandible to the parietal unit during mouth opening. Based on the highly movable connections between the parietal unit and occipital segment, this pull may contribute to ventral depression of the parietal unit. (iii) We consider that the PATS plays an important role in the metakinetic mechanism. During mouth opening, the parietal is depressed ventrally, which means that the PATS becomes deformed as its anterior end sitting firmly in the parietal bone is also bent ventrally. In this phase, it helps to guide downward rotation of the skull roof. During mouth closure, the PATS aids in stabilising the parietal unit in its dorsal resting position.

Limitations of the presented model

The presented model for squamate amphikinesis follows the tradition of Versluys, Frazzetta and later authors by using planar hypotheses to discuss different types of cranial kinesis. This means that streptostyly, mesokinesis and metakinesis are interpreted and modelled as rotational movements in the parasagittal plane over an axis running transversely through the skull. Skull manipulations presented in the present study basically followed planar rotational movements as suggested by the quadric-crank model. However, movements in other planes might occur during feeding as well, meaning that presented types of kinesis are presumably not as planar as suggested by the quadric-crank model. This aspect was beyond the scope of the present study and would require utilisation of experimental 3D data from modalities such as XROMM. This kind of data could provide multiplanar information on cranial mobility or even asymmetric movements during biting, for example, which may in future contribute to deepen our understanding of the lizard skull.

A functional hypothesis for the presented model of *A. kitaibelii* amphikinesis: metakinesis improves MAME function by reducing fibre strain

After formulating our extended model on lizard amphikinesis, we discuss its functional implications. Unlike the majority of past studies concerning lizard cranial kinesis, which focused mainly on streptostyly and mesokinesis, our considerations explicitly focus on metakinesis.

The MAME is a complex pennate muscle consisting of several portions inserting mainly on the coronoid bone of the mandible by the complex coronoid aponeurosis (Nash and Tanner, 1970; Wineski and Gans, 1984). Considering the length of the *A. kitaibelii* mandible from the anterior symphysis to the retroarticular process, the coronoid bone lies slightly posterior to the middle of the mandible (Fig. 1A). This means that the MAME has to be stretched considerably to achieve large gapes, although stretching is reduced by pennation. This is problematic, as overstretching of a muscle reduces its force production (Oatis, 2016). Since the early studies on lizard cranial kinesis, increase of gape was considered to be one of the adaptive advantages of a kinetic skull. This hypothesis was later rejected, as Frazzetta (1962) showed convincingly that, according to the quadric-crank model, amphikinesis theoretically could not increase gape. Although the

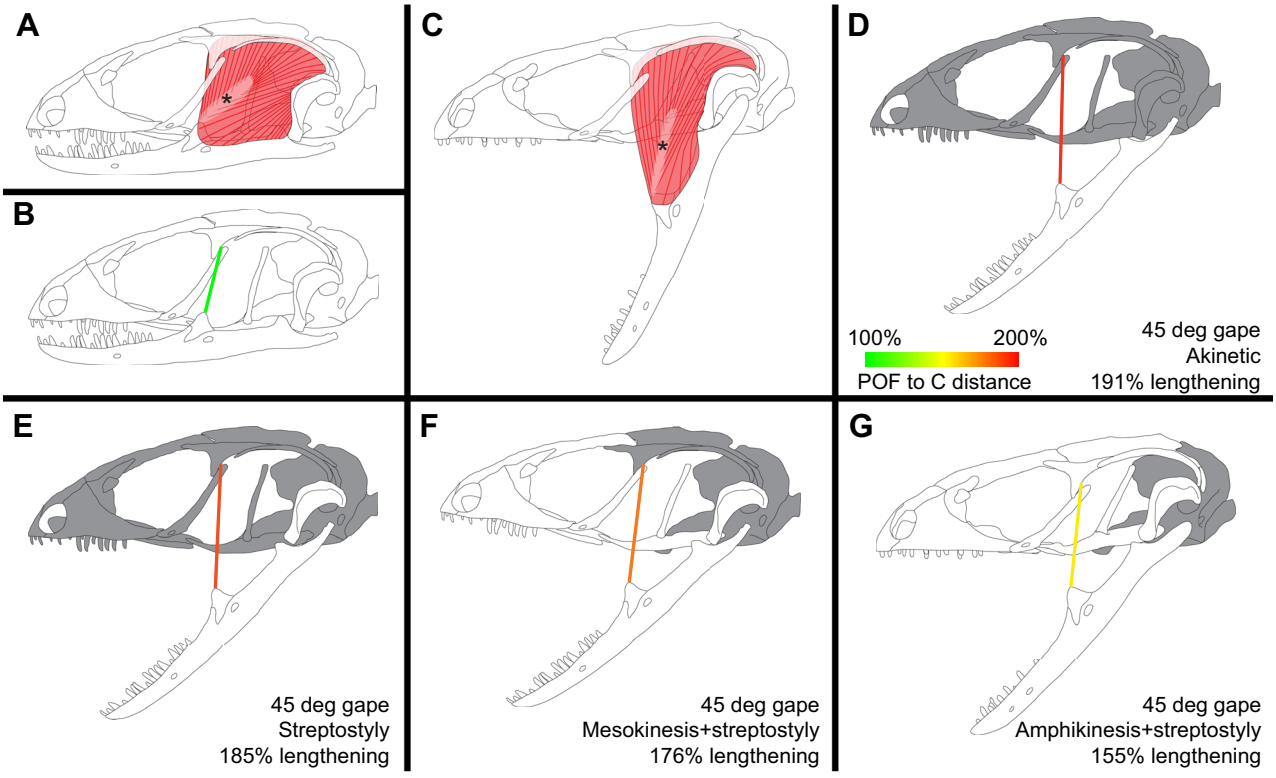

Fig. 7. A functional hypothesis for the amphikinetic lizard skull based on our observations on *A. kitaibelii*. According to our hypothesis, metakinesis (as part of the amphikinetic mechanism) brings the skull roof closer to the mandibles and thus allows the animal to achieve a certain mouth gape while reducing muscle strain in the external adductor muscles. This figure is based on simple 2D simulation of 45 deg mouth gape angle for different skull conditions. (A) Closed mouth, showing the course of muscle fibres of the external mandible adductors inserting either directly on the mandible or via the coronoid aponeurosis. (B) Distance between postorbitofrontal (POF) and coronoid (C) in resting position, roughly representing length and course of most anterior MAME fibres. (C) Opened mouth (skull manipulation, roughly 60 deg gape), showing course of muscle fibres of the external mandible adductors. Most anterior MAME fibres are stretched considerably. (D) Lengthening of the POF to C distance to 191% in a completely akinetic skull. (E) In a skull showing streptostyly, lengthening is reduced to 185%. (F) In a skull showing mesokinesis and streptostyly, lengthening is further reduced to 176%. (G) In a skull showing amphikinesis and streptostyly, lengthening is most strongly reduced to 155%. *Coronoid aponeurosis.

theoretical background of this conclusion was correct in light of the quadric-crank model, it did not take into account that muscle strain could be a severe practical constraint for achieving large mouth gapes. Thus, we here present a modified version of the gape hypothesis, which we call the 'MAME strain hypothesis'. Accordingly, metakinesis does not allow larger theoretical gapes, but it achieves a certain (large) gape with less stretching of the MAME fibres. If overstretching (muscle strain) is an important factor for MAME function, practical gape angle might be considerably increased by a movable parietal unit (metakinesis). The idea that metakinesis reduces MAME fibre strain represents a testable hypothesis, which can be addressed using modelling approaches. In a recent study, Lautenschlager (2015) used simulations to predict muscle strains in jaw opening in several extant and extinct archosaurs, assuming that 130% muscle fibre length (relative to resting length) would provide the optimal tension limit, whereas literature data on skeletal muscle architecture suggest that the maximum tension limit before fibres start to tear is 170% (Nigg and Herzog, 2007; Sherwood et al., 2012). Based on this model, the maximum gape angle for several archosaur species was estimated. A similar simulation could be also used for the lizard skull, and we performed a simplified and preliminary 2D simulation to test the plausibility of our MAME strain hypothesis (Fig. 7). In the first step, we measured fibre stretch in 3D at three different localities in the MAME based on microCT volumes from iodine-stained specimens (Fig. S5). Image resolution in microCT data allowed direct measurement of muscle fibre bundle lengths and orientations (Figs 3A and 6B). The three measured localities included muscle origins at the postorbitofrontal, squamosal and quadrate bone, respectively. From the three tested locations, the highest strain was measured in the most anterior MAME fibres originating from the postorbitofrontal (Fig. S5). These fibres are also the most vertical fibres of the MAME (Fig. 7A) and run almost perfectly in the parasagittal plane (Fig. 3A), and thus we considered this portion of the MAME to be the most suitable for our preliminary simulation. In the second step, we performed a 2D simulation for lengthening of the distance between the postorbitofrontal and coronoid (which is roughly the position of the most anterior MAME fibres) for a gape angle of 45 deg, which is close to the maximum observed gape angle during feeding cycles in *A. kitaibelii*. Simulation was conducted for four different hypothetical skull conditions: akinetic, streptostylic, streptostylic plus mesokinetic, and streptostylic plus amphikinetic. Results of this simplified and preliminary 2D simulation support our hypothesis that strain in MAME fibres might restrict practical gape angle in *A. kitaibelii*. Although the distance between the postorbitofrontal and coronoid is lengthened to 191% in an akinetic skull, lengthening is reduced with increasing degree of kinetic movements. In a skull showing only streptostyly, lengthening is still 185%, but additionally involving mesokinesis would reduce lengthening to 176%, and involving amphikinesis would reduce lengthening even further to 155% (Fig. 7D–G). It needs to be highlighted that the presented preliminary 2D simulations vastly simplify a complex anatomical problem. In order to draw a sound conclusion of MAME strain in kinetic and akinetic skulls, it would be necessary to analyse fibre stretch for the whole MAME in 3D. The presented data is intended to illustrate the MAME strain hypothesis: increasing cranial kinesis brings the skull roof closer to the mandible during mouth opening, thus reducing strain in the MAME. Finally, fibres experiencing the greatest stress may not be activated at the largest gape angles, allowing the lizard to actively modulate the use of different fibre bundles during feeding.

Although this preliminary analysis provides some support for the MAME strain hypothesis, future 3D simulations are needed to test this hypothesis in more detail for *A. kitaibelii* and also across a variety of kinetic and akinetic lizard taxa. Furthermore, simulations that consider angle of insertion of all muscle fibre bundles of the MAME would make it possible to model the stretched MAME performance for both a metakinetic and an akinetic skull roof. Muscle performance could then be evaluated at different gape angles for kinetic and akinetic skulls. We expect this kind of simulation to bring novel insights into the mechanisms and possible functional roles of cranial kinesis, as a metakinetic skull roof will not only decrease fibre stretching in the MAME but also change significantly the angle of MAME fibres with reference to the coronoid aponeurosis and mandible, thus yielding also a change in the MAME force vector. Next to computer simulations, the MAME strain hypothesis could be tested in comparative bite force studies, by measuring bite forces at different gape angles (e.g. 20, 30, 40 and 50 deg) for different kinetic and akinetic taxa. Accordingly, kinetic species should be able to retain muscle function at large gape angles, and thus bite force, much better than akinetic species. The current data on *A. kitaibelii* showed prolonged and reasonably hard biting at high gape (50 deg), which is in accordance with our hypothesis and the observed cranial kinesis in *A. kitaibelii*.

Conclusions

The miniaturised scincid *A. kitaibelii* has a kinetic skull showing both streptostyly and amphikinesis. We observed neither skull bone reduction nor a reduced ossification in dermal skull bones owing to miniaturisation, and skull design is similar compared with other small scincids such as *Chalcides* (Caputo, 2004) and *Trachylepis* (Paluh and Bauer, 2017). Our detailed morphological investigation focuses on the anatomical basis for metakinesis and includes morphological features and functional links that have not been previously discussed in that context (such as the paired anterolateral shelves of the parietal). Our observations lead us to formulate an extended functional model for lizard amphikinesis with a special emphasis on the functional advantage of metakinesis. We hypothesise that metakinesis is primarily a mechanism for improving MAME function. Metakinesis may help to avoid MAME fibre overstretching during mouth opening and appears to re-align fibres with reference to the coronoid aponeurosis. This hypothesis can be addressed and tested in future simulations and bite force studies. We conclude that new technical tools such as high-resolution microCT imaging and computer simulations will allow us to experimentally test the hypothesis concerning cranial kinesis also for small and even miniaturised species, for which data on cranial kinesis are most badly needed.

Acknowledgements

We thank Boyan Zlatkov and Silviya Georgieva for help with the catching of *Ablepharus kitaibelii* specimens. We also thank Yurii Kornilev for assisting with high-speed cinematography.

Competing interests

The authors declare no competing or financial interests.

Author contributions

Conceptualization: S.H., N.N., V.V.; Methodology: S.H., N.N., S.K., C.J.B., P.L., A.H., V.V.; Software: C.J.B., P.L.; Formal analysis: A.H.; Investigation: S.H., N.N., S.K., C.J.B., P.L., A.H., V.V.; Writing - original draft: S.H., P.L., A.H.; Writing - review & editing: S.H., N.N., C.J.B., P.L., A.H., V.V.; Visualization: S.H.; Project administration: S.H.

Funding

This research received no specific grant from any funding agency in the public, commercial or not-for-profit sectors.

Supplementary information

Supplementary information available online at
http://jeb.biologists.org/lookup/doi/10.1242/jeb.198291.supplemental

References

Arnold, E. (1998). Cranial kinesis in lizards: variations, uses, and origins. In *Evolutionary Biology*, Vol. 30 (ed. M. Hecht, R. Macintyre and M. Clegg), pp. 323-357. New York: Plenum Press.

Bock, W. J. (1964). Kinetics of the avian skull. *J. Morphol.* **114**, 1-41. doi:10.1002/jmor.1051140102

Bramble, D. M. and Wake, D. B. (1985). Feeding mechanics of lower tetrapods. In *Functional Vertebrate Mophology* (ed. M. Hildebrand, D. M. Bramble, K. F. Liem and D. B. Wake), pp. 230-261. Cambridge: Harvard University Press.

Buytaert, J., Goyens, J., De Greef, D., Aerts, P. and Dirckx, J. (2014). Volume shrinkage of bone, brain and muscle tissue in sample preparation for micro-CT and light sheet fluorescence microscopy (LSFM). *Microsc. Microanal.* **20**, 1208-1217. doi:10.1017/S1431927614001329

Caputo, V. (2004). The cranial osteology and dentition in the scincid lizards of the genus *Chalcides* (Reptilia, Scincidae). *Italian J. Zool.* **71**, 35-45. doi:10.1080/11250000409356604

Condon, K. (1987). A kinematic analysis of mesokinesis in the Nile monitor (*Varanus niloticus*). *Exp. Biol.* **47**, 73-87.

Condon, K. (1998). The anatomical basis of cranial kinesis in the Nile monitor. *Am. Zool.* **38**, 201A.

Daza, J. D., Abdala, V., Thomas, R. and Bauer, A. M. (2008). Skull Anatomy of the Miniaturized Gecko *Sphaerodactylus roosevelti* (Squamata: Gekkota). *J. Morphol.* **269**, 1340-1364. doi:10.1002/jmor.10664

De Vree, F. and Gans, C. (1987). Intracranial movements in *Gekko gecko* (Reptilia, Sauria). *Acta Anat.* **130**, 25-25.

De Vree, F. and Gans, C. (1994). Feeding in tetrapods. In *Advances in Comparative and Environmental Physiology: Biomechanics of Feeding in Vertebrates* (ed. V. L. Bels, M. Chardon and P. Vandewalle), Vol. 18, pp. 93-118. Berlin: Springer-Verlag.

Frazzetta, T. H. (1962). A functional consideration of cranial kinesis in lizards. *J. Morphol.* **111**, 287. doi:10.1002/jmor.1051110306

Frazzetta, T. H. (1966). Studies on the morphology and function of the skull in the Boidae (Serpentes). II. Morphology and function of the jaw apparatus in *Phython sebae* and *Python molurus*. *J. Morphol.* **118**, 217-295. doi:10.1002/jmor.1051180206

Frazzetta, T. H. (1983). Adaptation and function of cranial kinesis in reptiles: a time-motion analysis of feeding in alligator lizards. In *Advances in Herpetology and Evolutionary Biology: Essays in Honor of Ernest E. Williams* (ed. A. Rhodin and K. Miyata), pp. 222-244. Cambridge: Museum of Comparative Zoology.

Frazzetta, T. H. (1986). The origin of amphikinesis in lizards - a problem in functional-morphology and the evolution of adaptive systems. *Evol. Biol.* **20**, 419-461. doi:10.1007/978-1-4615-6983-1_8

Fuhn, I. E. (1969). Revision and redefinition of the genus *Ablepharus* Lichtenstein, 1823 (Reptilia, Scincidae). *Rev. Roum. Biol. Zool.* **14**, 23-41.

Gans, C. (1961). The feeding mechanism of snakes and its possible evolution. *Am. Zool.* **1**, 217-227. doi:10.1093/icb/1.2.217

Gans, C. (1974). *Biomechanics. An Approach to Vertebrate Biology*. Philadelphia: Lippincott Company.

Gingerich, P. (1971). Functional significance of mandibular translation in vertebrate jaw mechanics. *Postilla* **152**, 1-10.

Haas, G. (1935). Zum Bau des Primordialcraniums und des Kopfskelettes von *Ablepharus pannonicus*. *Acta Zool.* **16**, 409-429. doi:10.1111/j.1463-6395.1935.tb00668.x

Hedrick, T. L. (2008). Software techniques for two- and three-dimensional kinematic measurements of biological and biomimetic systems. *Bioinspir. Biomim.* **3**, 034001. doi:10.1088/1748-3182/3/3/034001

Herrel, A. and De Vree, F. (1999). Kinematics of intraoral transport and swallowing in the herbivorous lizard *Uromastix acanthinurus*. *J. Exp. Biol.* **202**, 1127-1137.

Herrel, A., Aerts, P. and De Vree, F. (1998). Static biting in lizards: functional morphology of the temporal ligaments. *J. Zool.* **244**, 135-143. doi:10.1111/j.1469-7998.1998.tb00015.x

Herrel, A., De Vree, F., Delheusy, V. and Gans, C. (1999). Cranial kinesis in gekkonid lizards. *J. Exp. Biol.* **202**, 3687-3698.

Herrel, A., Aerts, P. and De Vree, F. (2000). Cranial kinesis in geckoes: functional implications. *J. Exp. Biol.* **203**, 1415-1423.

Herrel, A., Schaerlaeken, V., Meyers, J. J., Metzger, K. A. and Ross, C. F. (2007). The evolution of cranial design and performance in squamates: consequences of skull-bone reduction on feeding behavior. *Integr. Comp. Biol.* **47**, 107-117. doi:10.1093/icb/icm014

Hofer, H. (1960). Vergleichende Untersuchungen am Schädel von *Tubinambis* und *Varanus* mit besonderer Berücksichtigung ihrer Kinetik. *Gegenb. Morphol. Jahrb.* **100**, 706-746.

Iordansky, N. N. (1966). Cranial kinesis in lizards: contribution to the problem of the adaptive significance of skull kinesis. *Zool. Zh.* **45**, 1398-1410 (in Russian, translation by Smithsonian Herpetological Service, 1968).

Iordansky, N. N. (1996). The temporal ligaments and their bearing on cranial kinesis in lizards. *J. Zool.* **239**, 167-175. doi:10.1111/j.1469-7998.1996.tb05444.x

Iordansky, N. N. (2011). Cranial kinesis in lizards (Lacertilia): origin, biomechanics, and evolution. *Biol. Bull.* **38**, 868-877. doi:10.1134/S1062359011090032

Johnston, P. (2010). The constrictor dorsalis musculature and basipterygoid articulation in *Sphenodon*. *J. Morphol.* **271**, 280-292. doi:10.1002/jmor.10797

Kardong, K. V. (1977). Kinesis of jaw apparatus during swallowing in cottonmouth snake, *Agkistrodon piscivorus*. *Copeia* **1977**, 338-348. doi:10.2307/1443913

Lautenschlager, S. (2015). Estimating cranial musculoskeletal constraints in theropod dinosaurs. *R. Soc. Open Sci.* **2**, 150495. doi:10.1098/rsos.150495

Limaye, A. (2012). Drishti, a volume exploration and presentation tool. Proc. SPIE 8506, *Developments in X-Ray Tomography VIII, 85060X*. doi:10.1117/12.935640

Ljubisavljević, K., Džukić, G. and Kalezić, M. L. (2002). Morphological differentiation of the Snake-eyed Skink *Ablepharus kitaibelii* (Bibron & Bory, 1833), in the north-western part of the species' range: systematic implications. *Herpetozoa* **14**, 107-121. doi:10.2478/asn-2018-0010

MacLean, W. (1974). Feeding and locomotor mechanisms of teiid lizards: functional morphology and evolution. *Pap. Avulsos Zool.* **27**, 179-213.

McBrayer, L. D. and White, T. D. (2002). Bite force, behavior, and electromyography in the teiid lizard, *Tupinambis teguixin*. *Copeia* 111-119. doi:10.1643/0045-8511(2002)002[0111:BFBAEI]2.0.CO;2

Metzger, K. (2002). Cranial kinesis in lepidosaurs: skulls in motion. In *Topics in Functional and Ecological Vertebrate Morphology* (ed. P. Aerts, K. D'Août, A. Herrel and R. Van Damme), pp. 15-46. Shaker Publishing.

Mezzasalma, M., Maio, N. and Guarino, F. M. (2014). To move or not to move: cranial joints in European gekkotans and lacertids, an osteological and histological perspective. *Anat. Rec.* **297**, 463-472. doi:10.1002/ar.22827

Montuelle, S. J. and Williams, S. H. (2015). In vivo measurement of mesokinesis in *Gekko gecko*: the role of cranial kinesis during gape display, feeding and biting. *PLoS ONE* **10**. doi:10.1371/journal.pone.0134710

Nash, D. F. and Tanner, W. W. (1970). A comparative study of the head and thoracic osteology and myology of the scinks *Eumeces gilberti* Van Denburgh and *Eumeces skiltonianus* (Baird and Girard). *Bringham Young Univ. Sci. Bull. Biol. Series* **XII**, 1-32.

Natchev, N., Heiss, E., Lemell, P., Stratev, D. and Weisgram, J. (2009). Analysis of prey capture and food transport kinematics in two Asian box turtles, *Cuora amboinensis* and *Cuora flavomarginata* (Chelonia, Geoemydidae), with emphasis on terrestrial feeding patterns. *Zoology* **112**, 113-127. doi:10.1016/j.zool.2008.05.002

Natchev, N., Tzankov, N., Vergilov, V., Kummer, S. and Handschuh, S. (2015). Functional morphology of a highly specialised pivot joint in the cranio-cervical complex of the minute lizard *Ablepharus kitaibelii* in relation to feeding ecology and behaviour. *Contrib. Zool.* **84**, 13-23. doi:10.1242/jeb.198291

Nigg, B. M. and Herzog, W. (2007). *Biomechanics of the Musculo-Skeletal System*. New York: Wiley.

Oatis, C. A. (2016). Biomechanics of skeletal muscle. In *Kinesiology: The Mechanics and Pathomechanics of Human Movement* (ed. C. A. Oatis), pp. 51-76. Philadelphia: Wolters Kluwer.

Paluh, D. J. and Bauer, A. M. (2017). Comparative skull anatomy of terrestrial and crevice-dwelling *Trachylepis* skinks (Squamata: Scincidae) with a survey of resources in scincid cranial osteology. *PLoS ONE* **12**, e0184414. doi:10.1371/journal.pone.0184414

Payne, S. L., Holliday, C. M. and Vickaryous, M. K. (2011). An osteological and histological investigation of cranial joints in geckos. *Anat. Rec. (Hoboken)* **294**, 399-405. doi:10.1002/ar.21329

Rieppel, O. (1978a). The phylogeny of cranial kinesis in lower vertebrates, with special reference to the Lacertilia. *N. Jb. Geol. Paläont. Abh.* **156**, 353-370.

Rieppel, O. (1978b). Streptostyly and muscle function in lizards. *Experientia* **34**, 776-777. doi:10.1007/BF01947321

Rieppel, O. (1979). A functional interpretation of the varanid dentition (Reptilia, Lacertilia, Varanidae). *Gegenb. Morphol. Jahrb.* **125**, 797-817.

Rieppel, O. (1984a). Miniaturization of the lizard skull: its functional and evolutionary implications. *Symp. Zool. Soc. London* **52**, 503-520.

Rieppel, O. (1984b). The upper temporal arcade of lizards-an ontogenetic problem. *Rev. Suisse Zool.* **91**, 475-482. doi:10.5962/bhl.part.81891

Rieppel, O. (1993). Patterns of diversity in the reptilian skull. In *The Skull*, Vol. 2. *Patterns of Structural and Systematic Diversity* (ed. J. Hanken and B. Hall), pp. 344-390. Chicago: University of Chicago Press.

Schwenk, K. (2000). Feeding in lepidosaurs. In *Feeding: Form, Function and Evolution in Tetrapod Vertebrates* (ed. K. Schwenk), pp. 175-291. San Diego: Academic Press.

Sherwood, L., Klandorf, H. and Yancey, P. (2012). Muscle physiology. In *Animal Physiology: From Genes to Organisms* (ed. L. Sherwood, H. Klandorf and P. Yancey), pp. 335-384. Belmont, CA: Brooks/Cole.

Smith, K. K. (1980). Mechanical significance of streptostyly in lizards. *Nature* **283**, 778-779. doi:10.1038/283778a0

Smith, K. K. (1982). An electromyographic study of the function of the jaw adducting muscles in *Varanus exanthematicus* (Varanidae). *J. Morphol.* **173**, 137-158. doi:10.1002/jmor.1051730203

Smith, K. K. and Hylander, W. L. (1985). Strain-gauge measurement of mesokinetic movement in the lizard *Varanus exanthematicus*. *J. Exp. Biol.* **114**, 53-70.

Starck, D. (1979). *Vergleichende Anatomie der Wirbeltiere auf evolutionsbiologischer Grundlage: Band 2: Das Skeletsystem: Allgemeines, Skeletsubstanzen, Skelet der Wirbeltiere einschliesslich Lokomotionstypen*. Berlin-Heidelberg-New York: Springer-Verlag.

Throckmorton, G. S. (1976). Oral food processing in two herbivorous lizards, *Iguana iguana* (Iguanidae) and *Uromastix aegyptius* (Agamidae). *J. Morphol.* **148**, 363-390. doi:10.1002/jmor.1051480307
Versluys, J. (1910). Streptostylie bei Dinosauriern. *Zool. Jb. Anat.* **30**, 175-260.
Versluys, J. (1912). Das Streptostylie-Problem und die Bewegungen im Schädel bei Sauropsiden. *Zool. Jb. Suppl.* **15**, 545-716.
Versluys, J. (1936). Kranium und Visceralskelett der Sauropsiden: 1. Reptilien. In *Handbuch der vergleichenden Anatomie der Wirbeltiere*, Vol. 4 (ed. L. Bolk, E. Göppert, E. Kallius and W. Lubosch), pp. 699-808. Wien: Urban und Schwarzenberg.
Ward, S. R. and Lieber, R. L. (2005). Density and hydration of fresh and fixed human skeletal muscle. *J. Biomech.* **38**, 2317-2320. doi:10.1016/j.jbiomech.2004.10.001
Wineski, L. E. and Gans, C. (1984). Morphological basis of the feeding mechanics in the shingle-back lizard *Trachydosaurus rugosus* (Scincidae, Reptilia). *J. Morphol.* **181**, 271-295. doi:10.1002/jmor.1051810303
Yildirim, E., Kumlutas, Y., Candan, K. and Ilgaz, C. (2017). Comparative skeletal osteology of three species of Scincid lizards (Genus: *Ablepharus*) from Turkey. *Vertebr. Zool.* **67**, 251-259.
Zusi, R. (1993). Patterns of diversity in the avian skull. In *The Skull*, Vol. 2. *Patterns of Structural and Systematic Diversity* (ed. J. Hanken and B. Hall), pp. 391-436. Chicago: Chicago University Press.
Zweers, G. (1982). The feeding system of the pigeon (*Columba livia* L). *Adv. Anat. Embryol. Cell Biol.* **73**, 1-104. doi:10.1007/978-3-642-68472-2_1